



## Earthquake Damage Detection in Built Environment: An Object-Oriented Approach Using Radar Imagery

*Babak Mansouri*

Risk Management Research Center,  
International Institute of Earthquake Engineering and Seismology, Tehran, Iran

(Received: April 1, 2013; Accepted in Revised Form: June 22, 2013)

**Abstract:** The feasibility to develop a rapid urban seismic damage detection procedure utilizing satellite radar imagery is investigated. In direct observation of city-wide building loss, remote sensing damage detection techniques have shown merits in rapid damage detection in urban areas. Remote sensing technology has the capability of extracting buildings in urban scenes. Comparing “before” and “after” images and benefiting from image processing techniques, it is possible to detect the extent of high hit zones. In detecting post-earthquake damages to buildings and in order to reduce detection errors and for minimizing the false alarms, it seems positive logic to apply the change detection algorithms only to the patches that correspond exactly to building footprints. For this purpose, urban database revealing the 3D reconstruction of the city is developed using parcels records. The parcels are extracted from aerial photos (stereography processing) then complemented and updated using VHR (very high resolution) optical satellite image (i.e. Quickbird imagery). The change detection algorithm and the calibration modeling are applied to “before” and “after” EnviSat SAR images considering only the building layer. The methodology is applied to the city of Bam and the associated building damages of its 2003 earthquake were emphasized. Results were compared with an independent direct visual damage interpretation using a VHR optical image.

**Key words:** Earthquake damage • Remote sensing • Satellite image • VHR optical image • Building damage

### INTRODUCTION

In order to assess the risk or loss of any specific building damages, it is necessary to create building geo-databases and to derive building vulnerability or loss of specific functions to building taxonomy. For the case of direct observation of loss, remote sensing damage detection techniques have shown merits in rapid damage detection in urban areas. Remote sensing in general has the capabilities of detecting some important phenomenon on the ground surface with minimal knowledge of the study area. However, ancillary site data help in reducing the errors and provide a base for validation and calibration of results. So far, pixel-based remote sensing methods have been exploited by different research groups in around the world and the basic image processing schemes have been well documented [1-3]. Also some

object-based (object-oriented) image processing algorithms were developed for the purpose of detecting and classifying objects (i.e. image segmentation) on the ground [4, 5]. For example, in urban areas where the post-earthquake physical damages to buildings are of interest, in order to reduce the detection errors and for minimizing the false alarms, it seems logical to apply the change detection algorithms only to the patches that correspond exactly to building footprints. This is even more crucial for the case of SAR image processing because SAR returns are strongly sensitive to the imagery geometry and features comprised within each pixel.

The feasibility of change/damage detection using civilian SAR satellites data with a ground resolution of about 20 meters (Envisat ASAR SLC image) is sought keeping in mind that the rapid advancement in such technologies will deliver much higher resolutions and

better abilities to detect changes. Very high resolution satellite SAR images are already accessible through the Radarsat2 (3m in fine mode) and Terrasarx (1m) systems and likely to be delivered for urban disaster applications.

For this research, Envisat satellite data was chosen because pre\_ and post\_event data were available for the Bam event. The sensor collected before- and after-event imagery of the Bam, Iran earthquake that occurred on December 26<sup>th</sup>, 2003. Two sets of “before” and one “after” SAR data are used. The change detection is based on the comparison of the presented SAR index as applied on building footprints using orbital information and the urban configuration in order to report the levels of change in different parcels. Such damage maps can potentially serve in disaster management and also in estimating urban economic losses. It is noted that in previous researches [1, 6] satisfactory results were achieved in identifying the regional location of collapsed buildings. Finally, a damage map that was obtained from a direct visual damage interpretation result is used to validate and calibrate these findings.

**MATERIALS AND METHODS**

Figure 1 depicts the major steps involved in this research. The parcel information are extracted from the aerial digital maps and stored into a GIS media. Radar data for before and after the event are co-registered and the SAR change index map is extracted. The change index map is used in a way that only building footprints are taken into account and the pixels corresponding to the rest of the features are filtered out. Also the proposed SAR index is calibrated based on the geometry of imagery by considering the most visible walls of each parcel. Because the SAR index is affected by the random noise, the city block layer was introduced so that the computed indices are averaged for the parcels within individual blocks.

**Change/damage Index:** The basic assumption for change detection using a repeat-pass interferometric data (single antenna but two image acquisitions) is that scene distances to the receiving antennas are practically the same. The interferometric phase is mainly affected by changes in the scattering behavior of the scene, or changes in the scene geometry. Interferometric data are used for creating SAR change index map. Table 1 lists the baseline information between the interferometric pairs as used in this research.

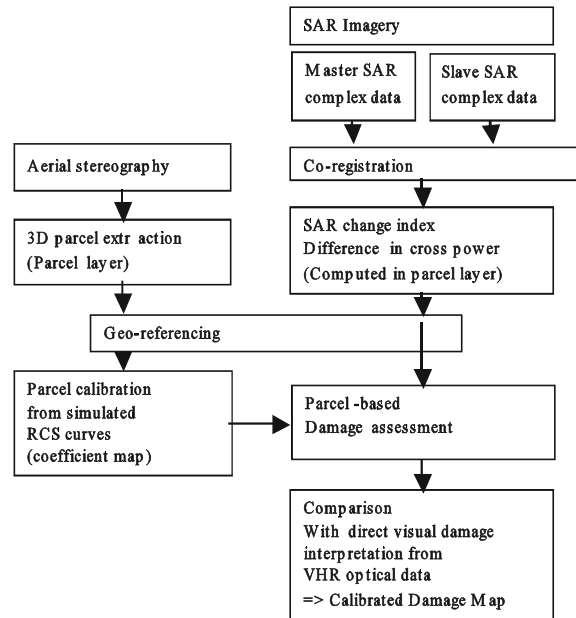


Fig. 1: Major steps involved in the algorithm

Table 1. Interferometric data pairs used in this study

Interferometric pairs	Sensor-target plane (m)	
	Baseline information	
	Normal	Parallel
June 11, 03 and Dec. 3, 03	473.21	147.98
June 11, 03 and Feb. 11, 04	476.12	133.22

$$\text{Coherence } (C_1, C_2) = \frac{|\sum C_1 C_2^*|}{\sqrt{(\sum C_1 C_1^*)(\sum C_2 C_2^*)}} \quad (1)$$

Equation (1) is defined as the coherence between two complex images; its nominator is defined as the cross-power (Xp). When the same image is used in the cross-power terms it is called the self-power (Sp) of the image. The summation is evaluated within a window of the size of 3 pixels (in range) by 15 pixels (in azimuth). Window computations allow for compensation of minute mis-registration of the data pairs and for the reduction of inherent noises, which often occur at the expense of reducing data resolution. It is best to compare before-before and before-after coherence maps and cross-power (Xp) maps that exhibit similar baseline correlations. The use of a common “before” dataset serves as a baseline image. Coherence maps reflect scene/object changes that are independent of the locality, largely because of the normalization terms in the denominator. For c ross-power, strong backscattering

(i.e. corner reflectors) changes are more pronounced and more suitable for urban damage assessment as used in this study

Nevertheless, the presence of false assignments, random objects (moving object such as cars) and also feature changes observed in the nature are unavoidable. Considering “before” and “after” images and summarizing the difference values of the calibrated Xp index for individual buildings a preliminary damage map is generated. This map is created considering the following main steps.

**Ancillary Data–Parcel Information:** The scope of present research is to compile high resolution city data with parcel level of details including the city topography and building height information and other attributed data. The parcel maps and building height information were mainly extracted from 1:2000 scale digital maps provided by National Cartographic Center (NCC) of Iran. These maps were created by processing aerial stereo-photographs. The extracted city parcel information have been processed and compiled from different sets of data that required both spatial adjustments and temporal change considerations. The parcel layer was complemented and updated using VHR (very high resolution) optical satellite image (i.e. Quickbird imagery). Figure 2 shows a portion of this data that has been GIS-ready and comprises of city parcel records pronouncing the building footprints and building heights.

**RCS (Radar Cross Section) Simulation:** In this section, a basis for SAR index calibration is discussed. Considering the fact that SAR sensor is side-looking and since the cross-power term indicates a measure of the SAR image intensity and the radar return is highly dependent on the geometry of the imaging; such index must be calibrated for the entire scene. Urban environments can essentially be represented by a combination of different geometrical shapes (i.e. rectangular plates). The Envisat SAR system is consistent with a monostatic measurement/simulation that is the transmitter and the receiver are regarded as the same antenna and located at the same position with respect to the scene. It is expected that after a building collapses, the backscattering coefficient of the image is drastically reduced. The RCS values of the objects are highly sensitive functions of the sensor-object observation and object azimuth angles. The walls of the buildings and their adjacent pavements formed dihedral corner reflector. The RCS simulation is completed for VV polarization



Fig. 2: A portion of the 1:2000 urban digital map comprising of parcel data

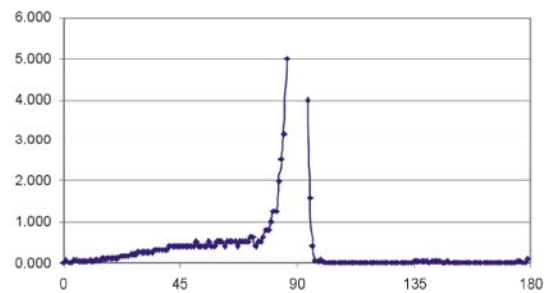


Fig. 3: VV polarization angle dependent RCS simulation curve for vertical dihedral reflector

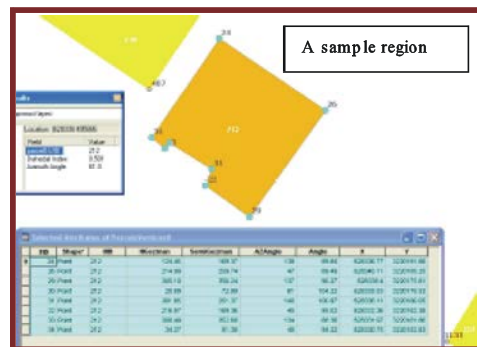


Fig. 4: Geo database analysis: detection of the most visible walls of the parcels (radar specific) [1]



Fig. 5: Parcel azimuth angle for the most visible walls (radar specific)

(specific to Envisat data) according to the vertical dihedral corner reflector and for one-degree increment in azimuth to cover the entire range. The effective area intercepting the beam is a function of the incident, the azimuth angles and also the intercepting area. Figure 3 is the simulated RCS value with respect to the azimuth angles.

**Implementation in GIS:** In order to apply the method for each parcel, the database (parcel records) was refined as to filter out all the buildings that are obscured. Moreover, analyzing each building footprint sides and corners; considering different angles, an automated process selects the most radar-detectable walls of the building. The corresponding azimuth angle is stored for each parcel record as shown in Figure 4. Then, the dedicated algorithm estimates the SAR signature based on the angle dependent RCS values for each parcel, then computes the calibration coefficients.

The azimuth angles are attributed for individual buildings (parcel record). Figure 5 shows the entire city of Bam; the optical very high resolution data as the base map and the color-coded parcels reflecting the azimuth angle of the most detectable walls in radar configuration. Angles around 82 degrees are close to the maximum radar reception in general since the satellite orbit is about 98 degrees near polar and the images are acquired in the descending pass.

## RESULTS AND DISCUSSION

Since the nature of the radar data is noisy and also coarse in term of resolution. A city block mask was also used in averaging the change detection results. Therefore, two masks namely the parcel layer and the block layer were used in tandem. The parcel layer reflects the calibration coefficients and the building block layer reflects the averaged SAR change index values. The result of the rapid damage detection algorithm of this research is shown in Figure 6; where two levels of damage severity were made detectable.

The feasibility of change detection is evaluated according to an independent ground truth method that is counting the damaged buildings manually. Yamazaki *et al.* [7] have created a damage map (Figure 7) for Bam by visual interpretation of the VHR Quickbird optical data. They have used the EMS-98 damage grades and the process of assigning different building damage grades was fully manual. Table 2 summarizes their results in addition to the assumed equivalent damage factor ranges according to ATC13 report.

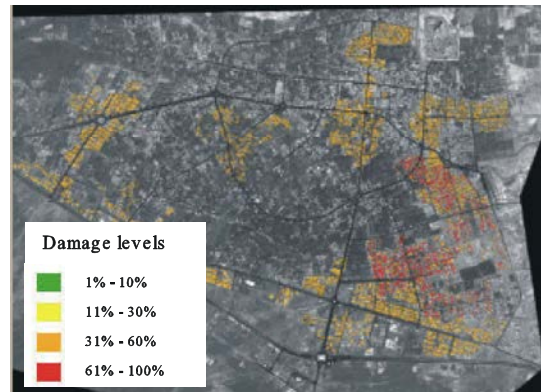


Fig. 6: Rapid SAR change detection results

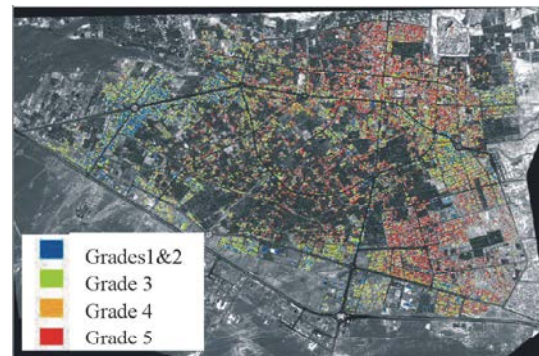


Fig. 7: SAR change detection by visual interpretation (courtesy of Yamazaki et al. [7])

Table 2: Visually interpreted damage grades and corresponding ATC13 damage factor

Damage grade assigned	No. of buildings interpreted	Assumed equivalent damage factor in ATC13	
		Range, %	Central, %
Grades 1& 2	1597	1-10	5
Grade 3	3815	10-30	20
Grade 4	1700	30-60	45
Grade 5	4951	60-100	80

Observing the rapid damage detection map of Figure 6 and comparing to the results illustrated in Figure 7, the major parts of hard hit zones were made feasible to detect with the expense of some existing false alarms. The coarse resolution of the SAR data that overlaps different features within each pixel and the presence of inherent noises within radar images in one hand and the complexity of the geometric configuration of urban settings with respect to radar detection on the other hand exhibit some limitation on the accuracy. However, for a rapid process of mapping hard hit zones right after large earthquakes in remote areas and for preliminary disaster management activities such as search and rescue, resource allocation the finding of such studies show



exceptional merits. It is emphasized that such modeling will be improved drastically by the use of very high resolution radar imageries.

#### **ACKNOWLEDGMENT**

This research was completed as part of a research contract between International Institute of Earthquake Engineering and Seismology with the municipality of Tehran (TDMMO) (contract # 190/503605). Professor Yamazaki is acknowledged for providing the authors with the visual damage interpretation data for the Bam earthquake.

#### **REFERENCES**

1. Mansouri, B., M. Shinozuka, C.K. Huyck and B. Houshmand, 2005. Earthquake-Induced Change Detection in Bam, Iran, by Complex Analysis Using Envisat ASAR Data. *Earthquake Spectra*, 1(21): 275.
2. Matsuoka, M. and F. Yamazaki, 2005. Building damage mapping of the 2003 Bam, Iran, earthquake using Envisat/ASAR intensity imagery. *Earthquake Spectra*, Special Issue. 1(21): 285.
3. Huyck, C.K., B.J. Adams, S. Cho, H. Chung and R.T. Eguchi, 2005. Towards rapid citywide damage mapping using neighborhood edge dissimilarities in very high-resolution optical satellite imagery – Application to the 2003 Bam, Iran earthquake. *Earthquake Spectra*, Special Issue. 1(21): 255.
4. Definiens Imaging, 2004. E-Cognition 4.0, User guide, Definiens Imaging GmbH, Munich, Germany.
5. Chen, Z. and T. Hutchinson, 2010. Probabilistic urban structural damage classification using bitemporal satellite images. *Earthquake Spectra*, 26(1): 87-109.
6. Mansouri, B. and M. Shinozuka, 2005. SAR image calibration by urban texture: Application to the BAM earthquake using Envisat satellite ASAR data. 3rd International Workshop on Remote Sensing for Post-Disaster Response, 12<sup>th</sup> and 13<sup>th</sup> September 2005, Chiba, Japan.
7. Yamazaki, F., Y. Yano and M. Matsuoka, 2005. Visual Damage Interpretation of Buildings in Bam City Using Quickbird Images Following the 2003 Bam, Iran, Earthquake. *Earthquake Spectra*, Special Issue 1(21): 329.